Int. J. Heat Mass Transfer. Vol. 29, No. 6, pp. 909–920, 1986
Printed in Great Britain

0017–9310/86 $3.00 + 0.00
Pergamon Journals Ltd.

Thermal conductivity of packed metal powders*

G. R. HADLEY
Fluid Mechanics and Heat Transfer Division, Sandia National Laboratories, Albuquerque, NM 87185, U.S.A.

(*Received* 17 *June* 1985 *and in final form* 17 *December* 1985)

Abstract—In this paper we present both experimental measurements and a theoretical model for the thermal conductivity of a consolidated mixture of two-metal powders. Measurements were made on samples of different mixture volume fractions at consolidations ranging from loose powder to above 90% theoretical density, using both air and water as saturants. We have applied the technique of volume averaging to produce working equations applicable to the general problem of thermal conduction through mixtures. Predictions made using these equations show good agreement with published two-phase data from a wide variety of sources.

1. INTRODUCTION

GRANULAR materials, both consolidated and unconsolidated, comprise an important class of constituents in modern engineering technology as well as in geophysical systems. Such constituents are found in explosives, chemical reactors, ceramics, and in naturally occurring soils and rocks, to name only a few. These composites range in complexity from relatively simple binary systems of packed spherical particles to agglomerates consisting of several irregularly-shaped constituents held together by porous cementing materials. Thus, modeling of mixtures continues to be a challenging endeavor of considerable complexity.

In this paper we describe an experimental and theoretical study of the conductive transfer of heat through those granular materials which may in some sense be considered 'random'. Thus we are leaving out laminar composites or systems with some built-in symmetry. In particular, we primarily will treat packed metal powders, although some theoretical comparisons with other granular data are presented. This specialization is made in an attempt to model a system whose components are well known and characterized. Thus the emphasis in this work will be on the development of theoretical models to predict the thermal conductivity of mixtures, rather than on measurements of systems of a particular practical interest.

The simple binary system consisting of unconsolidated (uncemented) particles of various shapes surrounded by a single pore fluid has been the subject of considerable study, resulting in a significant data base. This data is usually presented as plots of k_{eff}/k_f vs $\kappa \equiv k_m/k_f$, where k_{eff} is the effective conductivity of the mixture, k_m the matrix conductivity, and k_f that of the pore fluid. Recent work by Nozad *et al.* [1] has extended the range of κ to near 10^4 while providing a convenient synopsis of earlier work. Many theoretical models for the binary granular mixture have been proposed, ranging from empirical models [2] to the more fundamental work of Batchelor and O'Brien [3] and Jeffrey [4]. The reader is referred to Woodside and Messmer [5] for a good review of the modeling in this area prior to 1960.

For more complicated systems containing several phases, or phases which are connected with other than point contacts, little information is available. Woodside and Messmer [6] present measurements for sandstones which are of limited usefulness to the modeler due to uncertainties in the properties of the constituents. Nozad *et al.* [7] present useful measurements and numerical modeling for unconsolidated three-phase systems of which two of the phases are granular. The present work represents an attempt to treat both consolidated and unconsolidated systems using a single formalism.

2. EXPERIMENTAL APPARATUS

The thermal conductivity of various samples of pressed metal powder was measured using the steady-state comparator method. In this method one dimensional, steady-state heat flow is induced by maintaining a temperature gradient across a stack of cylindrical discs contained in a sample chamber. Assuming that the heat flux is identical in each disc, the conductivity of the unknown disc may be easily determined from measured temperature drops and the conductivity of a known standard disc.

The overall apparatus is shown in Fig. 1. The thermal comparator cell is contained in a pressure chamber fitted to provide various gas pressures from vacuum to 6.9 MPa (1000 p.s.i.). Temperature drops across the sample and the standard disc were obtained using miniature thermistors 0.35 mm in diameter, 3 mm in length with 0.025-mm-diameter enameled lead wires. All thermistors used in these experiments were first

* This work performed at Sandia National Laboratories supported by the U.S. Department of Energy under contract number DE-AC04-76DP00789.

NOMENCLATURE

A surface area [m^2]
f function defined by equation (19)
F heat flux [$W\ m^{-2}$]
k thermal conductivity [$W\ m^{-1}\ K^{-1}$]
n number of phases
$\hat{n}$ unit vector
T temperature [K]
V volume [m^3].

Greek symbols
α mixing parameter defined by equation (28)
δ percent theoretical density ($=1-\phi$)
κ k_m/k_f
ϕ volume fraction.

Subscripts
b brass
i phase
f fluid
m matrix
vac vacuum.

calibrated against a standard platinum RTD probe to a relative accuracy of 0.01 K using a constant temperature oil bath. This high accuracy temperature measurement capability allowed smaller temperature differences in the stack than is normally acceptable for good overall accuracy.

A schematic diagram of the thermal comparator cell is shown in Fig. 2. The stack was positioned in a nylon cylinder when the unknown was in powder form. For measurement of the 9.5-mm-thick solid discs, the nylon was removed and air acted as the radial insulation. Heat was supplied by a nichrome heater wire imbedded in the top aluminum disc, and removed from the bottom of the brass plug by a cold, temperature-regulated fluid circulating through copper coils wrapped around the plug. Dow Corning 304 heat sink compound was used between disc surfaces to reduce thermal contact resistance.

Thermistor placement for discs of low conductivity ($<15\ W\ m^{-1}\ K^{-1}$) was in 0.5-mm-deep grooves milled across a diameter on each face of both the unknown and standard discs. For discs of higher conductivity, the thermistors were inserted in 0.5-mm-diameter holes drilled 10 mm deep into the side of each disc. The holes were vertically aligned and 0.5 mm from each disc face. For measurements using powders, the top thermistors were positioned on the faces of the standard disc and copper cylinder.

Materials used for the standard discs were Dynasil 4000 glass and 304 stainless steel. The former has a conductivity of $1.37\ W\ m^{-1}\ K^{-1}$ and was used for unknown conductivities below about $15\ W\ m^{-1}\ K^{-1}$. The conductivity of the stainless standard was measured using the Dynasil disc and determined to be $13.6\ W\ m^{-1}\ K^{-1}$. The two discs were used to cover a range of conductivities from 0.037 to $113\ W\ m^{-1}\ K^{-1}$.

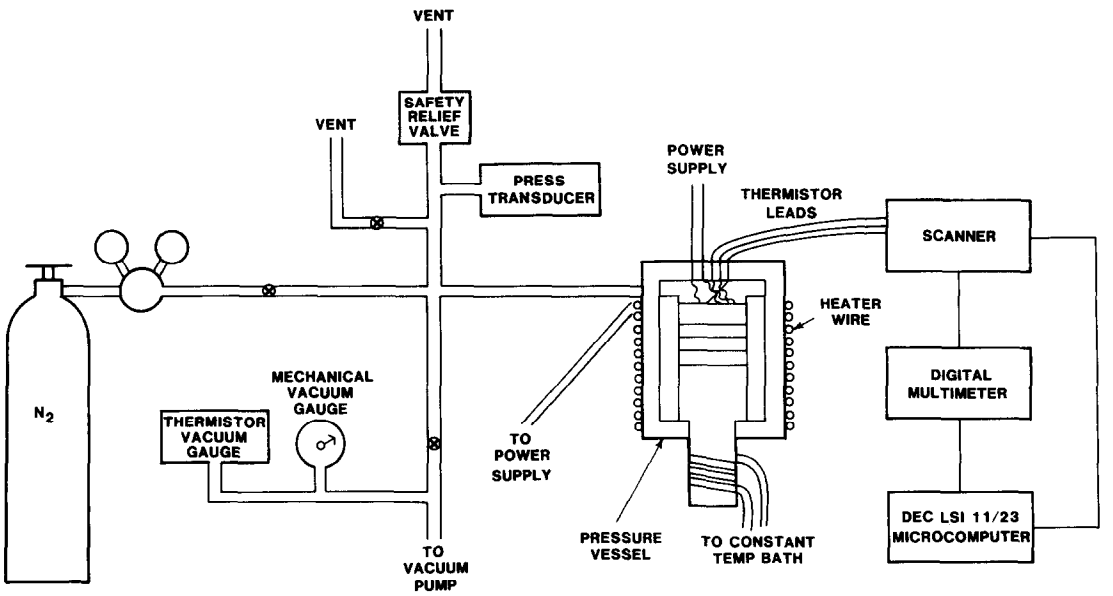

FIG. 1. Schematic diagram of the experimental apparatus.

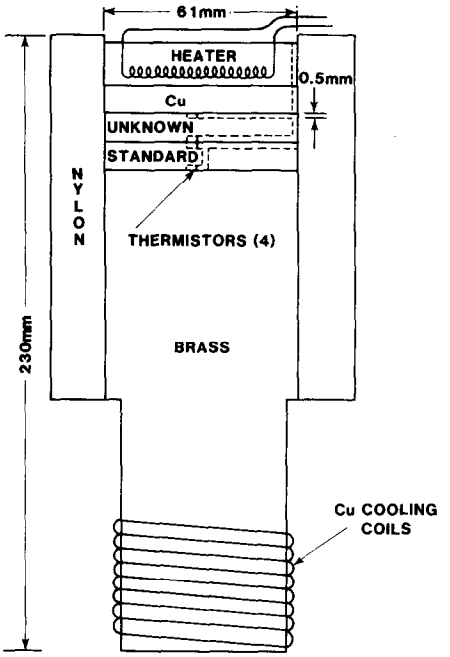

FIG. 2. Enlarged diagram of the thermal comparator cell. Heat flow is from top to bottom.

3. SAMPLE PREPARATION

All samples tested were prepared from mixtures of 70/30 brass powder and 316 stainless steel powder. Stainless steel powder samples were gas atomized (thus approximately spherical) whereas the brass powder used was highly angular. Because spherical powders do not press well, a different 316 stainless steel powder which was more angular was used for the pressed samples.

The solid samples resulted from cold pressing various mixtures of the two powders to percent theoretical densities (PTDs) ranging from 0.69 to 0.93. In order to include thermal conductivity data at a PTD of 1.0 (zero porosity), powder samples of each mix were hot-isostatic-processed at temperatures just below the melt point and pressures above 96.5 MPa (14,000 p.s.i.). These discs were found to have essentially zero porosity based on a measurement of density.

4. ESTIMATED MEASUREMENT ERROR

Measurement errors might be expected to occur in this experiment from a number of sources, including thermistor drift, radial heat loss, non-uniform contact resistance, and transient effects. These errors were minimized or eliminated both by careful design of the apparatus and frequent experimental checks during data acquisition. As a result, the measured values of conductivity listed in Table 2 are expected to be accurate to within $\pm 10\%$. This figure was arrived at by considering independently the sources of error discussed below, and is consistent with measurements made on the fully dense disc composed of 100% brass, which gave results accurate to within 7% of the accepted value for brass [8].

The major sources of error were determined to be non-uniform contact resistance and thermistor drift, together accounting for 80% of the stated uncertainty. Although the experiment was designed to be insensitive to a uniform contact resistance between discs, non-uniformity would lead to two-dimensional heat flow, thus violating the one-dimensional assumption needed for the derivation of the data reduction equations. This effect was minimized by the use of heat sink compound between all thermal contact paths. However, a comparison of measurements made on the same sample before and after disassembling the stack showed a spread of $\pm 5\%$, which we attribute to contact resistance effects. Thermistor drift was checked periodically by turning the heater off, and allowing the system to equilibrate thermally. The resulting temperature difference across a single disc was never larger than 0.025 K, and was more typically 0.01 K. Coupled with a minimum temperature difference across a disc during data acquisition of 0.4 K, this implies a maximum error of $\pm 7\%$. A more probable value of $\pm 3\%$ results from considering more typical temperature differences across the discs of >1.0 K, together with some additional allowance for calibration errors.

Other potential sources of error were of less significance. Uncertainties in thermistor location and finite thermistor size effects were expected to introduce errors of approximately $\pm 2\%$. Radial heat loss due to the natural convection of air around the stack was determined to be negligible by comparing a measurement of the conductivity of a fully-dense disc made under vacuum conditions with another made at high pressure. Transient effects were effectively eliminated by waiting until the attainment of a good steady state.

5. EXPERIMENTAL RESULTS

Results for the present measurements are summarized in Tables 1 and 2. Table 1 contains the thermal conductivity of the two metal constituents (determined by measurement) and the pore fluids (tabulated in [8]) at room temperature. The value for air includes a high pressure correction [9] of 5%. Table 2 contains the results of porosity and thermal conductivity measurements on the samples. The fourth and fifth columns are the weight percent and volume fraction of the brass

Table 1

Material	Thermal conductivity ($W\,m^{-1}\,K^{-1}$)
70/30 brass	113
316 ss	12.4
Water	0.6
Air or N_2 ($p = 2$ MPa)	0.0274

Table 2

No.	Sample form	Fluid	Weight % brass	ϕ_b	ϕ	k_{meas}	k_{theor}	% error
1	disc	air	100	1	0	113		
2	disc	air	80	0.784	0	61.7		
3	disc	air	60	0.577	0	36.1		
4	disc	air	40	0.380	0	24.4		
5	disc	air	20	0.187	0	17.3		
6	disc	air	0	0	0	12.4		
7	disc	vac	100	1.0	0.07	33.89		
8	disc	air	100	1.0	0.07	36.81	47.6	29
9	disc	vac	100	1.0	0.12	31.09		
10	disc	air	100	1.0	0.12	32.70	29.5	−10
11	disc	vac	100	1.0	0.18	17.90		
12	disc	air	100	1.0	0.18	20.51	18.0	−12
13	disc	vac	100	1.0	0.23	11.74		
14	disc	air	100	1.0	0.23	13.98	10.96	−22
15	disc	H_2O	100	1.0	0.23	28.07	24.9	−11
16	disc	vac	80	0.784	0.08	20.76		
17	disc	air	80	0.784	0.08	23.20	25.44	10
18	disc	vac	80	0.784	0.14	14.88		
19	disc	air	80	0.784	0.14	17.22	15.97	−7
20	disc	H_2O	80	0.784	0.14	29.15	30.5	5
21	disc	vac	80	0.784	0.19	12.78		
22	disc	air	80	0.784	0.19	14.71	10.83	−26
23	disc	vac	80	0.784	0.24	6.07		
24	disc	air	80	0.784	0.24	8.15	7.12	−13
25	disc	H_2O	80	0.784	0.24	16.38	18.0	10
26	disc	vac	60	0.577	0.10	12.95		
27	disc	air	60	0.577	0.10	13.92	14.56	5
28	disc	vac	60	0.577	0.15	9.11		
29	disc	air	60	0.577	0.15	11.28	9.5	−16
30	disc	vac	60	0.577	0.20	6.65		
31	disc	air	60	0.577	0.20	8.41	7.37	−12
32	disc	vac	60	0.577	0.26	4.30		
33	disc	air	60	0.577	0.26	5.92	4.26	−28
34	disc	vac	40	0.38	0.11	6.00		
35	disc	air	40	0.38	0.11	8.00	9.03	13
36	disc	vac	40	0.38	0.17	4.90		
37	disc	air	40	0.38	0.17	6.90	6.43	−7
38	disc	vac	40	0.38	0.22	3.89		
39	disc	air	40	0.38	0.22	5.71	4.29	−25
40	disc	vac	40	0.38	0.27	2.63		
41	disc	air	40	0.38	0.27	4.27	2.98	−30
42	disc	vac	20	0.187	0.12	3.78		
43	disc	air	20	0.187	0.12	5.80	5.78	0
44	disc	vac	20	0.187	0.18	2.61		
45	disc	air	20	0.187	0.18	4.52	3.80	−16
46	disc	vac	20	0.187	0.24	1.91		
47	disc	air	20	0.187	0.24	3.54	2.52	−29
48	disc	vac	20	0.187	0.29	1.39		
49	disc	air	20	0.187	0.29	2.82	1.65	−41
50	disc	H_2O	20	0.187	0.29	6.36	7.01	10
51	disc	vac	0	0	0.14	2.76		
52	disc	air	0	0	0.14	4.55	3.19	−30
53	disc	H_2O	0	0	0.14	6.89	8.04	17
54	disc	vac	0	0	0.20	1.72		
55	disc	air	0	0	0.20	3.38	2.07	−39
56	disc	vac	0	0	0.25	1.20		
57	disc	air	0	0	0.25	2.55	1.36	−46
58	disc	vac	0	0	0.31	0.81		
59	disc	air	0	0	0.31	2.00	0.75	−62
60	disc	H_2O	0	0	0.31	5.01	4.47	−11
61	powder	vac	100	1	0.60	0.0369		
62	powder	air	100	1	0.60	0.272	0.233	−14
63	powder	H_2O	100	1	0.60	4.76	4.29	−10
64	powder	vac	80	0.784	0.56	0.0431		
65	powder	air	80	0.784	0.56	0.296	0.248	−16
66	powder	vac	60	0.577	0.53	0.0473		
67	powder	air	60	0.577	0.53	0.316	0.252	−20
68	powder	vac	40	0.38	0.49	0.0424		
69	powder	air	40	0.38	0.49	0.294	0.271	−8
70	powder	vac	20	0.187	0.45	0.0666		
71	powder	air	20	0.187	0.45	0.332	0.292	−12
72	powder	vac	0	0	0.42	0.0588		
73	powder	air	0	0	0.42	0.331	0.275	−17
74	powder	H_2O	0	0	0.42	3.25	3.21	−1

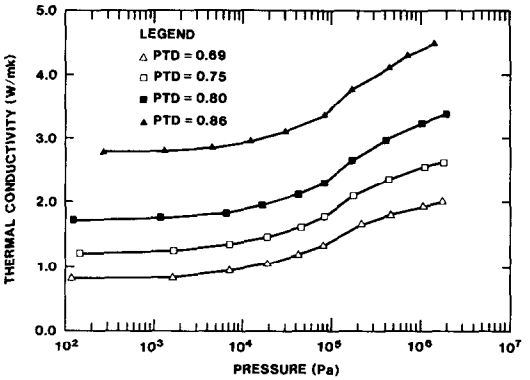

FIG. 3. Measured thermal conductivity of four pure stainless discs as a function of air pressure (PTD = percent theoretical density).

component, exclusive of voids. The sixth column gives the sample porosity. In the last three columns are listed the measured conductivity, a theoretical value determined from a model to be detailed later, and the percent discrepancy of the theoretical value from the experimental.

Note that, in Table 2, values obtained using air as the saturant are only reported for a pressure of 2 MPa, since only these values are of interest for modeling purposes. This conclusion follows from the fact that data for lower pressures would include effects due to 'molecular' conduction, because of the small pore sizes of samples used in this work [5]. In this regime, the effective conductivity of the fluid would vary spatially, depending on the gap width between metal surfaces. Such effects cannot be easily modeled by assuming a fluid of uniform conductivity. Nonetheless, measurements on most of the samples tested were made at a number of different pressures between vacuum and 2 MPa. Typical results are shown in Fig. 3 for four pure stainless steel discs of varying PTD. The shapes of the curves are similar to that reported by Woodside and Messmer [5]. Although these curves could be used to compute average pore size [5], that quantity was not of interest in this work.

In addition, vacuum measurements were made on six discs of identical composition and porosity. This was done partly as a check on measurement reproducibility, and partly to provide some estimate of the statistical sample-to-sample variation. The discs chosen were 20% brass with a porosity of 0.24. Measured thermal conductivities varied from a low of 1.91 $W\,m^{-1}\,K^{-1}$ to a high of 2.09 $W\,m^{-1}\,K^{-1}$, a spread of $\pm 5\%$. Thus sample uniformity was found to be better than the resolution of the measurements.

6. THEORY

6.1. *Basic volume averaging formalism*

Here we review the basic formalism of volume averaging [10, 11] in order to clarify notation and for the sake of completeness. We consider a multiphase mixture containing n phases, and construct an averaging volume which is large compared to the small-scale deviations in volume fraction of each component, but small enough so that all field variables (in this case temperature) vary only slightly over the volume. The shape of the averaging volume is assumed to be arbitrary and not to affect the results of any averaging operation. We associate with each averaging volume a point (which we denote the 'center') which shall serve to locate the volume with respect to the multiphase medium. Thus, spatial derivatives of volume-averaged quantities may be defined as the change in that quantity per unit distance movement of the averaging center, with the shape and orientation of the averaging volume fixed.

We now define the phase average of the field variable T over phase i as

$$\langle T_i \rangle \equiv \frac{1}{V} \int_{V_i} T \, dV \tag{1}$$

where V_i is the volume of phase i contained within the averaging volume V. Likewise the intrinsic phase average is defined by

$$\langle T_i \rangle^i \equiv \frac{1}{V_i} \int_{V_i} T \, dV. \tag{2}$$

In addition, we define a global average by integrating over all phases within V:

$$\langle T \rangle \equiv \frac{1}{V} \int_{V} T \, dV. \tag{3}$$

Examination of equations (1) and (3) shows that

$$\langle T \rangle = \sum_{i=1}^{n} \langle T_i \rangle. \tag{4}$$

Taking the gradient of each term in equation (4) and using the spatial averaging theorem of Slattery [12] to transform averages of gradients into gradients of averages produces

$$\nabla \langle T \rangle = \sum_{i=1}^{n} \langle \nabla T_i \rangle - \sum_{i=1}^{n} \frac{1}{V} \int_{A_{i0}} T \hat{n}_i \, dA, \tag{5}$$

where A_{i0} is the bounding surface of phase i, with the exclusion of that portion coincident with the surface of the averaging volume, and $\hat{n}_i$ is the outward unit normal. Since each element of surface area between the phases occurs in two integrals with oppositely-directed normals, and since the temperature is continuous across all boundaries, all the integrals in equation (5) cancel. Thus we are left with

$$\nabla \langle T \rangle = \sum_{i=1}^{n} \langle \nabla T_i \rangle. \tag{6}$$

Now, the heat flux within phase i is given by

$$\mathbf{F}_i = -\overleftrightarrow{k}_i \nabla T. \tag{7}$$

Volume averaging equation (7), and defining a global-averaged heat flux in a similar manner to that of

temperature, gives

$$\langle \mathbf{F} \rangle = \sum_{i=1}^{n} \langle \mathbf{F}_i \rangle = -\sum_{i=1}^{n} \vec{k}_i \langle \nabla T_i \rangle. \tag{8}$$

We then define an average thermal conductivity for the mixture through the relation

$$\langle \mathbf{F} \rangle \equiv -\vec{k} \nabla \langle T \rangle, \tag{9}$$

which leads immediately to

$$\vec{k} \nabla \langle T \rangle = \sum_{i=1}^{n} \vec{k}_i \langle \nabla T_i \rangle. \tag{10}$$

Since intrinsic averages of intensive variables such as temperature correspond more closely with measureable quantities than do phase averages, we rewrite equations (6) and (10) to produce the final working equations

$$\nabla \langle T \rangle = \sum_{i=1}^{n} \phi_i \langle \nabla T_i \rangle^i \tag{11}$$

$$\vec{k} \nabla \langle T \rangle = \sum_{i=1}^{n} \phi_i \vec{k}_i \langle \nabla T_i \rangle^i. \tag{12}$$

Equations (11) and (12) are quite general, but present a closure problem, since for n phases we have two equations and (for scalar conductivities) $n+1$ unknowns. Thus, the specification of different closure schemes will produce different mixture models consistent with the assumptions used to derive (11) and (12).

6.2. *Two-phase systems*

We next specialize equations (11) and (12) to the case of a two-phase system consisting of a porous material filled with pore fluid. If ϕ is the porosity of the porous matrix, then we have

$$\nabla \langle T \rangle = \phi \langle \nabla T_f \rangle^f + (1-\phi) \langle \nabla T_m \rangle^m \tag{13}$$

$$\frac{k}{k_f} \nabla \langle T \rangle = \phi \langle \nabla T_f \rangle^f + \frac{k_m}{k_f} (1-\phi) \langle \nabla T_m \rangle^m, \tag{14}$$

where 'f' and 'm' refer to fluid and matrix, respectively, and all thermal conductivities are assumed to be scalars. We now need one additional equation in order to close the system described by equations (13), (14). It is instructive to consider some simple choices for closure. For example, if we choose

$$\langle \nabla T_f \rangle^f = \kappa \langle \nabla T_m \rangle^m, \tag{15}$$

then we recover the formula for two materials in series relative to the direction of heat flow:

$$\frac{k}{k_f} = \frac{\kappa}{\phi\kappa + 1 - \phi}. \tag{16}$$

This formula represents the lowest possible mixture conductivity for a given porosity. On the other hand, if we use the closure relation

$$\langle \nabla T_f \rangle^f = \langle \nabla T_m \rangle^m \tag{17}$$

then we recover the parallel formula

$$\frac{k}{k_f} = \phi + (1-\phi)\kappa, \tag{18}$$

which represents the highest possible mixture conductivity. Consequently, any mixture model which depends only upon ϕ and κ may be represented by the general closure relation

$$\langle \nabla T_f \rangle^f = \{ f(\kappa, \phi) + \kappa [1 - f(\kappa, \phi)] \} \langle \nabla T_m \rangle^m, \tag{19}$$

where the values of the function f range between zero and unity.

Two special systems were treated long ago by Maxwell [13] and merit examination at this point. The first is a dilute suspension of spherical particles in an infinite uniform fluid. For this system the mixture conductivity is

$$\frac{k}{k_f} = \frac{2\phi + \kappa(3-2\phi)}{3 - \phi + \kappa\phi}. \tag{20}$$

One may easily verify that this formula (which we will call the 'lower Maxwell' formula) is obtained by the closure choice $f = 2/3$. The second system, a solid body containing a dilute 'suspension' of fluid-filled voids, possesses a mixture conductivity (designated here the 'upper Maxwell' formula)

$$\frac{k}{k_f} = \frac{2\kappa^2(1-\phi) + (1+2\phi)\kappa}{(2+\phi)\kappa + 1 - \phi}. \tag{21}$$

One may verify that equation (21) is obtained from the closure choice

$$f = \frac{2\kappa}{2\kappa + 1}. \tag{22}$$

Hashin and Shtrikman [14] have shown that the two Maxwell formulas (20) and (21) are the most stringent upper and lower bounds for homogeneous, isotropic, two-phase mixtures. For this class of mixtures we may thus further restrict the values of f to be

$$\frac{2}{3} < f < \frac{2\kappa}{2\kappa + 1}. \tag{23}$$

The lower Maxwell formula (20) was derived by assuming that the solid spheres were too far apart to interact in any way, and thus is only valid in the limit $\phi \to 1$. Numerous attempts have been made to extend Maxwell's calculation to higher orders of $(1-\phi)$. Considerable success has resulted for the case of periodic arrays of spheres [15–17] but for random suspensions the success has been much more limited. After expending considerable effort, Jeffrey [18] produced a formula valid to second order in $(1-\phi)$, but the complicated analysis he used offers little hope of extending the calculation to higher orders. Consequently, a semi-empirical approach is taken here, by examining possible closure schemes.

Considerable insight into possible choices for the function f for real materials may be gained by examining the limit $\kappa \to \infty$ of some of the preceding

formulas. In this limit the matrix conductivity may be thought of as approaching infinity while the fluid conductivity remains constant. As long as the matrix is noncontiguous, it is obvious that the mixture conductivity must approach a constant, since the fluid conductivity limits that of the mixture. Once the matrix becomes contiguous, however, the mixture conductivity must increase without bound, being proportional to k_m, or κ. This limiting behavior is evidenced by the Maxwell formulas, for which

$$\lim_{\kappa\to\infty}\left.\frac{k}{k_f}\right|_{LM}=\frac{3-2\phi}{\phi} \tag{24}$$

$$\lim_{\kappa\to\infty}\left.\frac{k}{k_f}\right|_{UM}=2\kappa\frac{1-\phi}{2+\phi}. \tag{25}$$

We next examine the mixture result obtained from the averaging theory with arbitrary f:

$$\frac{k}{k_f}=\frac{\phi f+\kappa(1-\phi f)}{1-\phi(1-f)+\kappa\phi(1-f)}. \tag{26}$$

For $f=f(\phi)$, equation (26) has the limit

$$\lim_{\kappa\to\infty}\frac{k}{k_f}=\frac{1-\phi f}{\phi(1-f)}. \tag{27}$$

In addition, the value of this limit is monotone increasing with f. Thus, it appears that a suspension of particles which do not touch may be approximately modeled by using a function f which is independent of κ and monotone increasing with $1-\phi$ starting from the value 2/3. Unfortunately, not enough data exists in this regime to allow even a guess at the proper functional form.

As the porosity of a suspension decreases, a point will be reached at which the solid particles touch. These so-called 'granular' materials occur often in nature, and numerous efforts have been made to model the conductivity of such materials. Good reviews of this former work have been provided by Woodside and Messmer [5]. In a more recent paper, Batchelor and O'Brien [19] have modeled granular systems by adding on a term representing the 'contact' contribution to obtain the total mixture formula. We intend to adopt a similar approach here, by combining an expression appropriate to conduction through a contiguous solid (the upper Maxwell formula) with one appropriate to a suspension of particles [equation (26) with $f=f_0$ and $f_0>2/3$]. Thus we model a two-phase system where the solid phase is connected with the formula

$$\frac{k}{k_f}=(1-\alpha)\frac{\phi f_0+\kappa(1-\phi f_0)}{1-\phi(1-f_0)+\kappa\phi(1-f_0)}+\alpha\frac{2\kappa^2(1-\phi)+(1+2\phi)\kappa}{(2+\phi)\kappa+1-\phi} \tag{28}$$

where α and f_0 are to be determined. The parameter f_0 is expected to be approximately constant for a contiguous solid, whereas α will depend strongly on what may be called the 'degree of consolidation'. For granular systems α is small and the first term in (28) is dominant for moderate values of κ. For consolidated materials, however, α is moderate and the second term may be dominant over most of the range of κ. The validity of equation (28) will be checked against available data in a later section.

6.3. *Three-phase systems*

Here we take $n=3$ in equations (11) and (12) to get

$$\nabla\langle T\rangle=\phi_1\langle\nabla T_1\rangle^1+\phi_2\langle\nabla T_2\rangle^2+\phi_3\langle\nabla T_3\rangle^3 \tag{29}$$

$$k\nabla\langle T\rangle=k_1\phi_1\langle\nabla T_1\rangle^1+k_2\phi_2\langle\nabla T_2\rangle^2+k_3\phi_3\langle\nabla T_3\rangle^3 \tag{30}$$

where, as before, the conductivity has been reduced to a scalar. We next proceed to show that the three-phase system described by (29) and (30) can be formally decomposed into two two-phase problems, each requiring a single closure relation. Once this has been established, the methods developed in the previous section may be utilized in the solution of three-phase problems.

The decomposition proceeds by defining an intermediate temperature gradient and conductivity by

$$\langle\nabla T_i\rangle^i(\phi_1+\phi_2)\equiv\phi_1\langle\nabla T_1\rangle^1+\phi_2\langle\nabla T_2\rangle^2 \tag{31}$$

$$k_i\langle\nabla T_i\rangle^i(\phi_1+\phi_2)\equiv k_1\phi_1\langle\nabla T_1\rangle^1+k_2\phi_2\langle\nabla T_2\rangle^2. \tag{32}$$

Clearly, equations (31) and (32) describe a two-phase problem identical in form to equations (13) and (14) with porosities

$$\phi_i'=\frac{\phi_i}{\phi_1+\phi_2},\quad i=1,2. \tag{33}$$

The remaining equations become, with (31) and (32) inserted,

$$\nabla\langle T\rangle=(\phi_1+\phi_2)\langle\nabla T_i\rangle^i+\phi_3\langle\nabla T_3\rangle^3 \tag{34}$$

$$k\nabla\langle T\rangle=k_i(\phi_1+\phi_2)\langle\nabla T_i\rangle^i+k_3\phi_3\langle\nabla T_3\rangle^3. \tag{35}$$

Thus we see that components 1 and 2 have been combined into an intermediate component with conductivity k_i and porosity $\phi_1+\phi_2$. The latter then forms a two-phase system with component 3 as shown in equations (34) and (35) in a manner which is formally identical to that of equations (31) and (32). Thus we have succeeded in formally decomposing the three-phase problem described by equations (29) and (30) into two two-phase problems, each of which requires a single closure relation.

The above procedure demonstrates that the intuitively appealing idea of decomposing the three-phase problem into two two-phase problems is in fact rigorous, provided the two-phase problems are solved properly. The usefulness of this procedure thus depends entirely on one's ability to solve the two-phase problems. A judicious choice of pairing of phases is then that for which the resulting two-phase problems are as familiar and tractable as possible. For example, a granular mixture consisting of two solid constituents

should be decomposed by dealing first with the two solids and then the equivalent granular problem, since the latter is a familiar one which has a significant data base. This, in fact, is the approach we shall follow in attempting to model the three-phase experiments discussed in this paper.

Other applications appear to be possible for the three-phase decomposition presented here. Granular materials with thin oxide layers could be modeled by dealing first with the effect of the oxide coating on the matrix material. This might be treated by assuming the oxide to be in series with the matrix (since any heat flowing through the matrix must of necessity flow through the oxide layer). The conductivity of a granular material containing small amounts of water might also be amenable to treatment, since the water is known to reside in the immediate vicinity of grain contact points. The same formalism is of course generalizable to more than three phases so long as the constituent two- or three-phase component problems are solvable.

7. THEORETICAL COMPARISONS

7.1. *Comparison with present three-phase data*

Modeling of the data presented in this work will begin by attempting to represent the two metals by a single phase with an effective conductivity, as mentioned above. This then constitutes the first two-phase problem of the decomposition. To aid in this effort, we first plot the data for the consolidated discs vs percent theoretical density (PTD) in Fig. 4. The latter quantity is also designated by the symbol δ and is defined as the ratio of the average sample density to the average matrix density. From this definition, neglecting the density of air, it follows that

$$\delta = 1-\phi, \tag{36}$$

where ϕ is the sample porosity. Each curve in Fig. 4 corresponds to a particular mixture of the two metal constituents. Useful information may be obtained from Fig. 4 by considering the ratio of the conductivity at some brass volume fraction ϕ_b to that for pure brass at the same value of δ. This ratio has been plotted in Fig. 5, and serves to aid in the choice of a model for the mixture conductivity of the metal phases. The uncertainty is large for the points plotted, because they represent the ratio of two measured values. Nonetheless, it is clear that the fully consolidated ($\delta = 1$) discs do not follow the same mixture model as do the discs with lower PTD.

Theoretical predictions for the mixture using different closure models are shown in Fig. 5. The two solid lines are the upper and lower Maxwell curves discussed in Section 6. The upper curve results from the choice

$$f = \frac{2\kappa}{2\kappa+1} = 0.948 \tag{37}$$

and the lower from $f = 2/3$. [Both curves were obtained using equation (28) with $\alpha = 0$.] The dotted line is a simple linear weighting, equivalent to $f = 1.0$. The present data illustrates well the remarks made by Hashin [20] to the effect that a single formula depending only on void fraction and constituent properties may not be expected to reproduce all experimental results. Although the present data is not of sufficient accuracy to unambiguously distinguish between models, it appears that the fully dense data more closely follows the lower Maxwell curve, and the data at $\delta = 0.75$ corresponds approximately with the upper Maxwell curve. The best attempt at a model would therefore seem to be a simple parameterization for f of the form

$$f = \min \begin{cases} 0.948 \\ 1.605 - 0.938\delta \end{cases} \tag{38}$$

which is chosen to give $f = 2/3$ at $\delta = 1$, and $f = 0.948$ at $\delta \leqslant 0.7$. The cutoff at $f = 0.948$ occurs because the upper Maxwell curve is known to represent a maximum for homogeneous and isotropic systems.

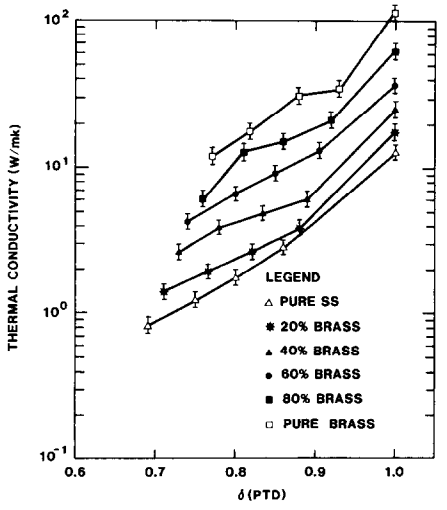

FIG. 4. Measured thermal conductivity of solid discs. Each curve corresponds to fixed weight percent of brass.

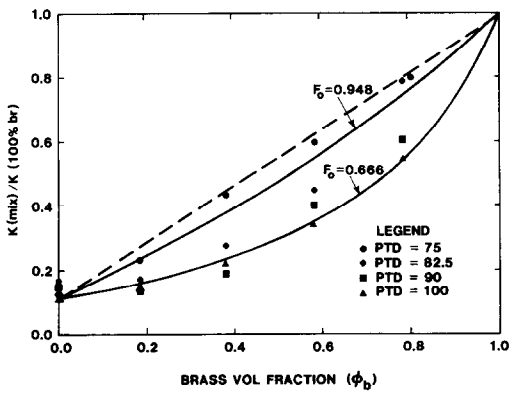

FIG. 5. Measured thermal conductivity of a solid disc of arbitrary composition relative to that of a pure brass disc with the same PTD. The two solid curves are the two Maxwell formulas.

The closure choice (38) thus specifies the result of the first two-phase problem, giving an effective metal conductivity for all samples tested. Note that results from the powder mixtures have not been included in the analysis thus far. This is because, for the powders, effects due to changing contact areas far outweigh effects due to changes in matrix conductivity. Thus the mixture model for the powder will be assumed to be the same as for the low PTD discs, i.e. $f = 0.948$.

Having an effective matrix conductivity model, we now turn to the second two-phase problem, that of the porous solid. We will model this problem using equation (28), with values for α and f_0 determined from experiment. We see that the use of vacuum as a pore fluid corresponds to $\kappa \to \infty$ in equation (28). Thus the conductivity at low gas pressure is predicted from (28) to be

$$\frac{k_{vac}}{k_m} = 2\alpha \frac{1-\phi}{2+\phi}. \tag{39}$$

Thus a measurement of conductivity made with pore pressures low enough to eliminate the influence of the pore fluid will provide a value for α. Figure 6 shows values of α obtained from equation (39) plotted vs δ (PTD). It thus appears that, for the samples tested here, α depends primarily upon material porosity and is approximately independent of other parameters such as particle shape or brass volume fraction. (Of course, the influence of particle shape may be implicitly included by its effect on porosity.) Whether the curve shown is valid for other systems remains to be determined.

Values of α for the consolidated discs are seen to lie below 0.4 even for values of δ as high as 0.92. Apparently, even in these highly compressed samples, heat flow paths are significantly affected by the remaining voids. Data for the powders shows clearly the important effect of particle contact. Powder mixes containing higher brass volume fractions packed to the lowest PTDs and possessed lower thermal conductivities, even though the matrix value for brass is over nine times that of stainless steel. This is presumably because the highly angular brass particles offer a lower number of contact points, or equivalently, a lower contact surface area than the mostly spherical stainless steel particles. Values for α thus range over 2.5 orders of magnitude, and seem to comprise a reasonably well-defined curve for both solids and powders. In the comparisons with experiment that follow, α will be determined from the curve shown in Fig. 6, even for data obtained from previous work. It is probable, however, that predictions for consolidated materials other than the type of packed metal powders presented here, would require separate vacuum measurements in order to determine the parameter α. This follows from the fact that the theory can be sensitive to this parameter, which, because it mirrors the effectiveness of particle contact, cannot always be predicted *a priori*.

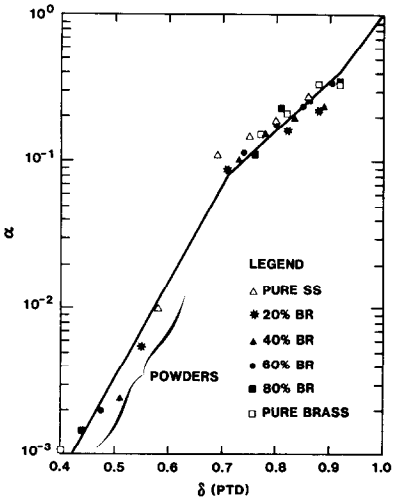

FIG. 6. Values of the consolidation parameter α determined from experimental measurements of evacuated samples. The curve represents an approximate fit.

The remaining parameter f_0 needed to complete the model is best determined from measurements made using a higher conductivity pore fluid such as water. In this case κ is moderate and the influence of the second term in equation (28) is reduced so that maximum sensitivity to f_0 is obtained. For the eight samples which were measured using water as the pore fluid, f_0 was found to range from 0.8 for stainless steel samples to 0.9 for pure brass samples. It is not understood why the angular brass particles should require a higher value of f_0 than the more spherical stainless steel. However, these eight results were fit to within an average error of $\pm 9\%$ using the simple linear formula

$$f_0 = 0.8 + 0.1\phi_b. \tag{40}$$

Comparisons between experimental values presented in this work and the present theory [with parameters as specified in equations (38), (40) and Fig. 6] are given in Table 2 with water and high pressure air as the pore fluids. The model fits the data to within an average error of $\pm 18\%$. If, instead of using the curve in Fig. 6, a unique value of α is determined from equation (39) for each sample, the average error drops to $\pm 16\%$. Alternatively, the replacement of equation (40) by a constant value of 0.9 for f_0 increases the error to $\pm 20\%$. In general, α is the most sensitive parameter in the theory, as it scales the matrix conduction component.

7.2. *Comparison with previous two-phase measurements*

The usefulness of a mixture theory such as the one presented here lies in its applicability to diverse systems which may differ from each other in certain aspects. Such a comparison may often reveal the importance of variables otherwise thought to be unimportant. Consequently, the present theory has been used to predict the results for a wide variety of measurements. For convenience, the large number of two-phase experiments compiled and catalogued by Crane and

Vachon [21] was chosen for comparison. These authors compared six different theories (including their own) with this body of data, thus making it an ideal test for the present model. Whereas Crane and Vachon's results were obtained by fitting the data with an unknown function of κ and ϕ, we have relied entirely on parameter values obtained from experiments described in this paper. Thus, values of α were taken from the curve in Fig. 6, with the identification $\delta = 1 - \phi$. For simplicity we have set $f_0 = 0.8$, a value consistent with spherical particles. The results are shown in Fig. 7 as theoretical values plotted against measured values. In addition to the experiments compiled by Crane and Vachon, the present two- and three-phase data have been included as well, so that this comparison includes values of thermal conductivity ranging over nearly three orders of magnitude. The parallel lines represent 20% deviations from unity. Overall, the comparison with Crane and Vachon's list of data is fair, giving an average error of $\pm 29\%$. The worst agreement occurs with the data of Kannaluik and Martin [22] for which the theory consistently overpredicts the measured values, sometimes by as much as a factor of 3. Further examination of Kannaluik and Martin's data reveals that their measurements were made on fine powders with the pores containing gases at atmospheric pressure or below. As these authors point out, molecular conduction effects are expected to have been present, particularly for the cases involving hydrogen gas, which should require special theoretical treatment. Consequently, we would expect Kannaluik and Martin's data to be overpredicted by simple two-phase models, and therefore it should not have been included in Crane and Vachon's list. Fountain and West's data [23] offer an extreme example of the same problem, and have not been considered at all in the present comparison. It is not clear to this author whether Crane and Vachon included them in their modeling attempts, though the data were listed and referenced. The exclusion of Kannaluik and Martin's data from the present comparison then reduces the average error to $\pm 22\%$, not substantially greater than that encountered when modeling the data presented in this work. It is also very close to the figure of $\pm 21\%$ published by Crane and Vachon for their model, although whether this figure would have improved had they omitted Kannaluik and Martin's data is unknown.

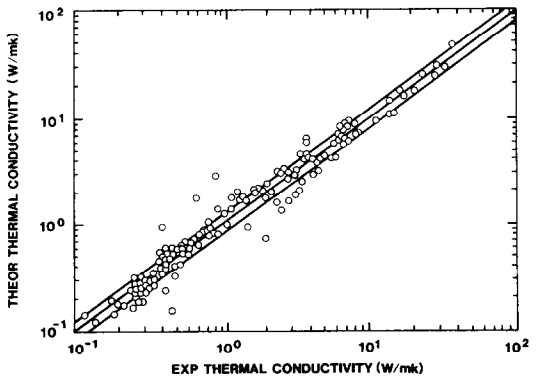

FIG. 7. Thermal conductivities determined from the present model vs measured values for a large sampling of previously published two-phase data as well as the present three-phase data.

7.3. *Comparison with other numerical calculations*

Another useful comparison may be made between the theory presented here and the numerical calculations of Nozad *et al.* [1] for two-phase granular materials. Nozad's calculations model the granular material as a periodic array of matrix blocks connected by slender 'bridges' of matrix material. For a bridge area equal to 2% of the block area these authors find good agreement with the majority of published data, as shown in Fig. 8 (reprinted from ref. [1]). (Most of the data shown in Fig. 8 are represented in Crane and Vachon's list.) Since the parameter α defined in the present work represents the fraction of heat conducted through matrix contact only, one would expect there to be a relationship between α and the relative 'bridge' area fraction of Nozad *et al.* That this appears to be the case may be seen in Fig. 8 where the present theory with $\alpha = 0.02$ (appropriate for $\phi = 0.38$) produces a curve remarkably close to Nozad's throughout the range of κ values. Although the exact agreement between the two parameters is probably fortuitous, the close correspondence between the calculations does help illuminate the basis of the present model.

8. CONCLUSIONS

In this paper we have presented both data and a theoretical model for the thermal conductivity of a consolidated mixture of metal powders. Although the literature abounds with data for two-phase granular systems (a single matrix material), data for three-phase systems is virtually nonexistent for cases where the constituent properties are well known. In addition there is little data available for two- or three-phase consolidated materials made up of well-characterized constituents. Herein we have presented data for such systems, where the percent theoretical density was varied in a systematic way from the lowest value which rendered the sample machinable to the highest value attainable with the available press. Mixture fraction of the two metals was also varied in stages, thus giving a useful parameter matrix for study.

We have applied the technique of volume averaging to produce two basic working equations applicable to the general problem of thermal conduction through mixtures. Several simple closure relations were examined (some of which yield well-known mixture models) until one was found which is useful in the modeling of two-phase granular mixtures. The more complex three-phase problem was shown to reduce formally to two two-phase problems (in agreement with one's intuition) together with three undetermined

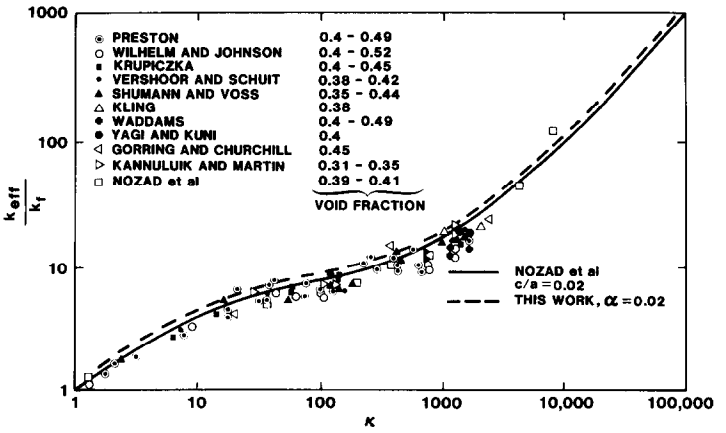

FIG. 8. Comparison of the present model with the numerical calculations of Nozad *et al.* [1] and previous two-phase data.

functions. These functions were determined by measurements made with evacuated samples, and samples saturated with water. Predictions were then made for 38 samples containing either water or high pressure air, so that they do not represent fits of these functions, but (except for the eight water-saturated measurements) are clear predictions employing no adjustable parameters. The data presented here was then modeled to within an average error of $\pm 18\%$.

In order to test the usefulness of the present theory, comparisons were made with a large body of two-phase data compiled by Crane and Vachon [21]. For these comparisons no changes were made in the values of the closure functions or the parameter α from those values predetermined by the present data. With the exclusion of Kannaluik and Martin's data, the predicted values for over 140 data points were within an average spread of $\pm 22\%$ of measured values. Thus we have presented a useful theory which is capable of predicting the conductivity of both two- and three-phase systems, whether granular or consolidated.

REFERENCES

1. I. Nozad, R. G. Carbonell and S. Whitaker, Heat conduction in multiphase systems I. Theory and experiment for two-phase systems, *Chem. Engng Sci.* **40,** 843–856 (1985).
2. K. Lichteneker, *Phys. Z.* **27,** 115–158 (1926).
3. G. K. Batchelor and R. W. O'Brien, Thermal or electrical conduction through a granular material, *Proc. R. Soc.* **A355,** 313–333 (1977).
4. D. J. Jeffrey, Conduction through a random suspension of spheres, *Proc. R. Soc.* **A335,** 355–367 (1973).
5. W. Woodside and J. H. Messmer, Thermal conductivity of porous media. I. Unconsolidated sands, *J. appl. Phys.* **32,** 1688–1699 (1961).
6. W. Woodside and J. H. Messmer, Thermal conductivity of porous media. II. Consolidated rocks, *J. appl. Phys.* **32,** 1699–1706 (1961).
7. I. Nozad, R. G. Carbonell and S. Whitaker, Heat conduction in multiphase systems. II. Experimental methods and results for three phase systems, *Chem. Engng Sci.* **40,** 857–863 (1985).
8. E. R. G. Eckert and R. M. Drake, Jr., *Analysis of Heat and Mass Transfer*, p. 774. McGraw-Hill, New York (1977).
9. R. C. Reed, J. M. Prausnitz and T. K. Sherwood, *The Properties of Gases and Liquids*, 3rd edn, p. 504. McGraw-Hill, New York (1977).
10. S. Whitaker, Diffusion and dispersion in porous media, *A.I.Ch.E. Jl* **13,** 420–427 (1967).
11. J. C. Slattery, Two phase flow through porous media, *A.I.Ch.E. Jl* **16,** 345–352 (1970).
12. J. C. Slattery, *Momentum, Energy and Mass Transfer in Continua*, p. 191. McGraw-Hill, New York (1972).
13. J. C. Maxwell, *A Treatise on Electricity and Magnetism*, 3rd edn, Vol. 1, p. 440. Clarendon Press, Oxford (1904).
14. Z. Hashin and S. Shtrikman, A variational approach to the theory of the effective magnetic permeability of multiphase materials, *J. appl. Phys.* **33,** 3125–3131 (1962).
15. R. C. McPhedran and D. R. McKenzie, The conductivity of lattices of spheres I. The simple cubic lattice, *Proc. R. Soc.* **A359,** 45–63 (1978).
16. D. R. McKenzie, R. C. McPhedran and G. H. Derrick, The conductivity of lattices of spheres II. The body-centered and face-centered cubic lattices, *Proc. R. Soc.* **A362,** 211–232 (1978).
17. A. A. Zick, Heat conduction through periodic arrays of spheres. *Int. J. Heat Mass Transfer* **26,** 465–469 (1983).
18. D. J. Jeffrey, Conduction through a random suspension of spheres, *Proc. R. Soc.* **A335,** 355–367 (1973).
19. G. K. Batchelor, F. R. S. and R. W. O'Brien, Thermal or electrical conduction through a granular material, *Proc. R. Soc.* **A355,** 313–333 (1977).
20. Z. Hashin, Assessment of the self-consistent scheme approximation: Conductivity of particulate composites, *J. Composite Mater.* **2,** 284–300 (1968).
21. R. A. Crane and R. I. Vachon, A prediction of the bounds on the effective thermal conductivity of granular materials, *Int. J. Heat Mass Transfer* **20,** 711–723 (1977).
22. W. G. Kannaluik and L. H. Martin, Conduction of heat in powders, *Proc. R. Soc.* **A141,** 144 (1933).
23. J. A. Fountain and E. A. West, Thermal conductivity of particulate basalt as a function of density in simulated lunar and martian environments, *J. geophys. Res.* **75,** 4063 (1970).

CONDUCTIVITE THERMIQUE DE POUDRES METALLIQUES COMPACTEES

Résumé—On présente à la fois les expériences et le modèle théorique pour la conductivité thermique d'un mélange consolidé de deux poudres métalliques. Les mesures sont faites sur des échantillons de différentes fractions volumiques de mélange jusqu'à 90% de la densité théorique, en utilisant l'air ou l'eau comme saturant. On applique la technique de la moyenne par le volume pour obtenir des équations utilisables pour le problème général de la conduction thermique à travers des mélanges. Les prévisions obtenues à partir des équations montrent un bon accord avec les données diphasiques publiées dans plusieurs sources.

DIE WÄRMELEITFÄHIGKEIT VON VERDICHTETEN METALLPULVERN

Zusammenfassung—In dieser Arbeit werden sowohl experimentelle Ergebnisse als auch ein theoretisches Modell für die Wärmeleitfähigkeit von verdichteten Mischungen aus zwei Metallpulvern vorgestellt. Messungen wurden an Proben von Mischungen unterschiedlicher Volumenanteile durchgeführt, wobei die Verdichtung von losem Pulver bis zu 90% der theoretischen Dichte reichte. Sowohl Luft als auch Wasser wurde als Sättigungsmittel benutzt. Die Technik der Volumenmittelung wurde angewandt, um Gebrauchsgleichungen zu entwickeln, die auf generelle Probleme der Wärmeleitung durch Mischungen angewendet werden können. Berechnungen, die mit diesen Gleichungen angestellt wurden, zeigten eine gute Übereinstimmung mit veröffentlichten Zweistoff-Daten aus den verschiedensten Quellen.

ТЕПЛОПРОВОДНОСТЬ ПЛОТНЫХ МЕТАЛЛИЧЕСКИХ ПОРОШКОВ

Аннотация—Представлены экспериментальные измерения и теоретическая модель теплопроводности уплотненной смеси двух металлических порошков. Измерения проведены на образцах с различным объемным содержанием компонентов при уплотнениях в диапазоне от сыпучего порошка до значений, достигающих 90% от максимально возможной плотности при использовании в качестве насыщающего вещества воздуха и воды. Методика объемного осреднения применяется для вывода уравнений, используемых в общей задаче теплопроводности в смесях. Расчеты, проведенные по этим уравнениям, показали хорошее соответствие с данными многих авторов.